Available online at www.sciencedirect.com
SCIENCE DIRECT
Tetrahedron 62 (2006) 6707–6717
Tetrahedron

Conformationally controlled (entropy effects), stereoselective vibrational quenching of singlet oxygen in the oxidative cleavage of oxazolidinone-functionalized enecarbamates through solvent and temperature variations

J. Sivaguru,[a] Marissa R. Solomon,[a] Hideaki Saito,[a,c,d] Thomas Poon,[e] Steffen Jockusch,[a] Waldemar Adam,[f,g] Yoshihisa Inoue[c,d] and Nicholas J. Turro[a,b,*]

[a]*The Department of Chemistry, Columbia University, New York, NY 10027, USA*
[b]*The Department of Chemical Engineering, Columbia University, New York, NY 10027, USA*
[c]*The Department of Applied Chemistry, Osaka University, 2-1 Yamada-oka, Suita 565-0871, Japan*
[d]*The Entropy Control Project, ICORP, JST, 4-6-3 Kamishinden, Toyonaka 560-0085, Japan*
[e]*Joint Science Department, W. M. Keck Science Center, 925 North Mills Avenue, Claremont McKenna, Pitzer, and Scripps Colleges, Claremont, CA 91711, USA*
[f]*Institute für Organische Chemie, Universität Würzburg, D-97074 Würzburg, Germany*
[g]*The Department of Chemistry, University of Puerto Rico, Facundo Bueso 110, Rio Piedras, PR 00931, USA*

Received 8 November 2005; revised 3 January 2006; accepted 13 January 2006
Available online 5 June 2006

We dedicate this work to our appreciated friend and distinguished colleague, Professor Sigfried Huenig (University of Wuerzburg), on the occasion of his 85th birthday

Abstract—On photooxygenation (methylene blue as sensitizer) of *E*/*Z* enecarbamates, equipped with the oxazolidinone chiral auxiliary, the oxidative cleavage of the alkenyl functionality releases the enantiomerically enriched methyldesoxybenzoin (MDB) product. The *extent* (% ee) as well as the *sense* (*R* vs *S*) of the stereoselectivity in the MDB formation depends on the choice of the alkene configuration; the efficacy of stereocontrol may be tuned by appropriate solvent and temperature conditions. Highlighted is the finding that the formation of the preferred MDB enantiomer (*R* or *S*) depends for the *E isomer* on the chosen solvent and temperature, but not for the corresponding *Z* isomer. The activation parameters for the various solvents disclose that differential entropy effects ($\Delta\Delta S^{\ddagger}$) dominate the conformationally more flexible *E* diastereomers. As mechanistic rationale for this unprecedented conformationally imposed stereochemical behavior, we propose the competitive action of stereoselective vibrational quenching of the attacking singlet oxygen by the enecarbamate versus sterically controlled stereoselective oxidative cleavage of its double bond.

1. Introduction

The success in achieving a high enantioselectivity in photochemical reactions[1–3] depends on how effectively the spatial requirements of the process are manipulated within the short lifetimes of the excited states.[4] To imprint stereocontrol in the photoproduct, organized assemblies[5–10] have been employed with varying degrees of success; however, obtaining a high enantioselectivity in solution still constitutes a formidable challenge.[1–3] In this regard, a novel concept, which we have explored in the stereoselective photooxidative cleavage of chiral enecarbamates, involves selective deactivation (quenching) of one of the diastereomers in a pair of chiral excited states.[11,12] Indeed, a high degree of stereocontrol may be imprinted in the photoproduct, but depending on the oxidant and the reaction conditions, the sense of the stereoselectivity may be reversed (Scheme 1).[11–13]

Previously we have shown[14–16] that such a photooxidative cleavage of enecarbamates actually entails a photooxygenation reaction,[17–20] in which the diastereomerically pure [1′*S*,2′*S*] dioxetane intervenes, as exemplified for the chiral *Z*-configured enecarbamates in Figure 1. The salient reactivity feature in the exposed snapshot is the preferential

Keywords: Chiral auxiliary; Conformational effects; *E*/*Z* isomers; Mechanism; Photooxygenation; Substituent effects; Stereoselectivity; Vibrational quenching.
* Corresponding author. Tel.: +1 212 854 2175; fax: +1 212 932 1289; e-mail: njt3@columbia.edu

0040–4020/$ - see front matter © 2006 Elsevier Ltd. All rights reserved.
doi:10.1016/j.tet.2006.01.119

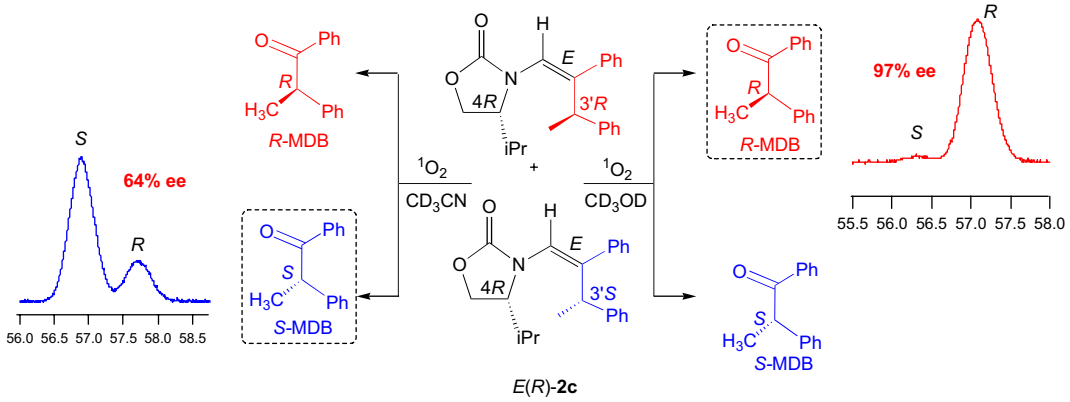

Scheme 1. Stereoselective photooxidative cleavage of oxazolidinone-functionalized *E*-enecarbamates.

quenching of the electronically excited $^1O_2$ as it attacks from below, such that in addition to the steric preference for the approach of $^1O_2$ from above, the synergistic interplay of quenching and steric hindrance dictates the observed high diastereoselectivity. Moreover, the stereoselection in the dioxetane formation is independent of the configuration at the C-3′ position of the alkyl side chain and the size of the alkyl substituent at the C-4 position of the oxazolidinone chiral auxiliary. Both, the methyl as well as the isopropyl derivatives 1′*Z*,4*R*(Me),3′*S*-**2b** and 1′*Z*,4*R*(*i*Pr),3′*R*-**2c** afford the corresponding [1′*S*,2′*S*] dioxetanes in diastereomeric ratios (dr) of about 95:5. For comparison, the enecarbamate *Z*-**2a** without a substituent at the C-4 position of the oxazolidinone, i.e., the parent ring, displays no diastereoselectivity whatsoever in the dioxetane formation of the [2+2] cycloaddition with $^1O_2$.[14–16]

In the present work, for comparison with the *Z* diastereomer, we have explored the photooxidative cleavage of the *E*-**2** enecarbamates (see the structure matrix of Chart 1). These are equipped with the oxazolidinone chiral auxiliary for asymmetric induction, to yield MDB and **3** as photoproducts (Scheme 2).[11,12] Analogous to the previously studied *Z* isomer,[14–16,21] ca. 50:50 diastereomeric mixtures of the *R*/*S* isomers at the C-3′ position in the alkene side chain were used, to assess how effective the stereocontrol would be in the kinetic resolution. These derivatives constitute versatile and informative substrates for the study of conformational, electronic, stereoelectronic, and steric effects on the stereoselectivity in the photooxidation of the alkene functionality.[11,12,14–16,21] Methylene blue was used to generate the singlet oxygen for the photooxidative cleavage of the alkenyl functionality in these chiral enecarbamates to produce the optically active MDB product.

The extent of and the sense in the enantioselectivity were assessed for the *E* geometry of the alkene as function of (a) the alkyl substituent at the C-4 position of the oxazolidinone chiral auxiliary (see Chart 1), (b) the configuration of the alkyl substituent at the C-4 position of the oxazolidinone chiral auxiliary, (c) the solvent, and (e) the reaction temperature. Herewith we report the results of this extensive investigation, which evidently show that the difference in the spatial arrangement offered by the *E* versus *Z* diastereomers of the enecarbamates is crucial. Furthermore, for achieving the observed high stereoselectivity in the formation of the MDB product during the photooxygenation of the *E* enecarbamates, we conjecture that the singlet oxygen is preferentially deactivated (quenched) in one of the epimeric transition structures for the *E*-enecarbamate/$^1O_2$ encounter complexes. Such selective quenching of diastereomeric excited states constitutes a promising *stereochemical tool*

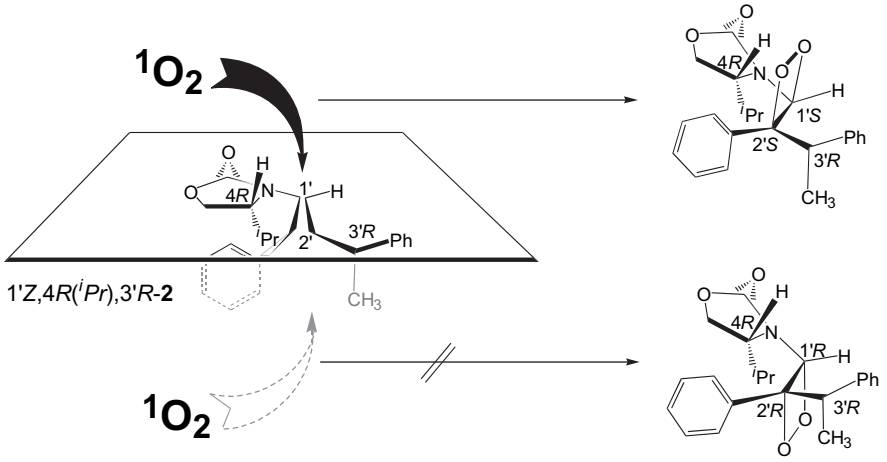

Figure 1. Preferred π-facial attack of $^1O_2$ from above controlled by the steric shielding of the 4-isopropyloxazolidinone substituent in the *Z* enecarbamates.

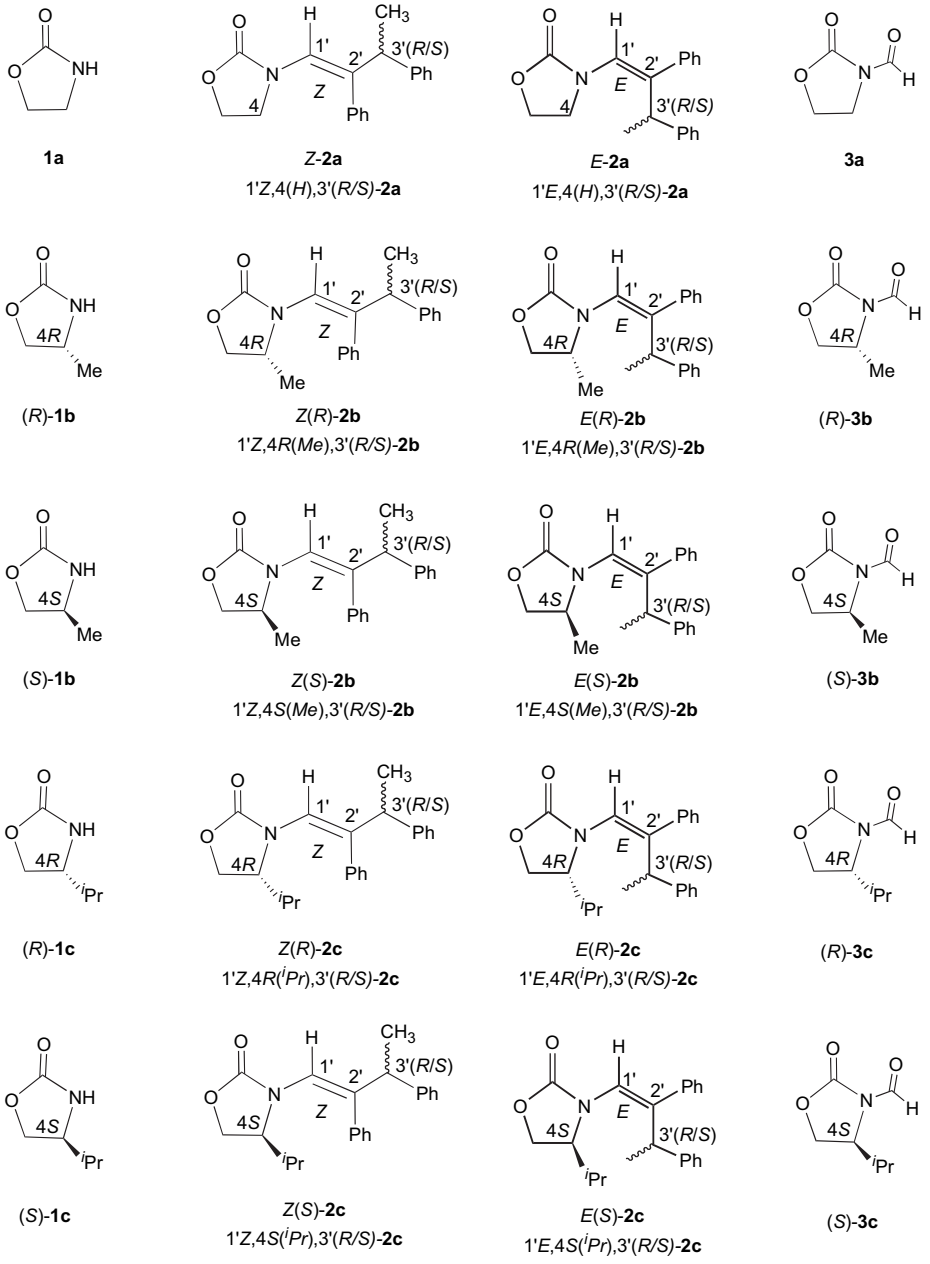

Chart 1. Structure matrix.

to effect the enantioselective photooxidative cleavage of chiral alkenes.

2. Experimental

2.1. Materials

All regular solvents were purchased from Aldrich and the deuterated solvents from Cambridge Isotope Labs and used as received. $CDCl_3$ was stored over sodium bicarbonate prior to use. Flash chromatography was carried out on silica gel, while 2-mm thick silica gel plates (EMD 60F) were employed for preparative TLC. Commercially available compounds were purified by standard procedures. The *Z*-**2** enecarbamates were synthesized by a previously published procedure.[11,12,14–16]

2.2. Methods

2.2.1. General procedure for the synthesis of the *E* enecarbamates *E*-2. A sample of 0.150 mmol of *Z*-**2** (see Chart 1, Scheme 2) was dissolved in 20 mL of CH_2Cl_2 and placed into a quartz test tube, fitted with a rubber septum, gas delivery needle, and vent needle. The solution was purged for 20 min with dry N_2 gas and then irradiated at 254 nm in a Rayonet photochemical reactor for 20–30 min under a positive N_2 pressure. GC analysis of the photolysate showed that the photostationary state (*Z*/*E*=52:48) was reached after 20 min. The solvent was removed at ca. 25 °C and 15 Torr on a rotatory evaporator. The residue was loaded onto a preparative TLC plate and eluted with a 2:1 mixture of hexane and methyl *tert*-butyl ether (MTBE). The faster running fraction was extracted with a 1:1 mixture of CH_2Cl_2 and EtOAc

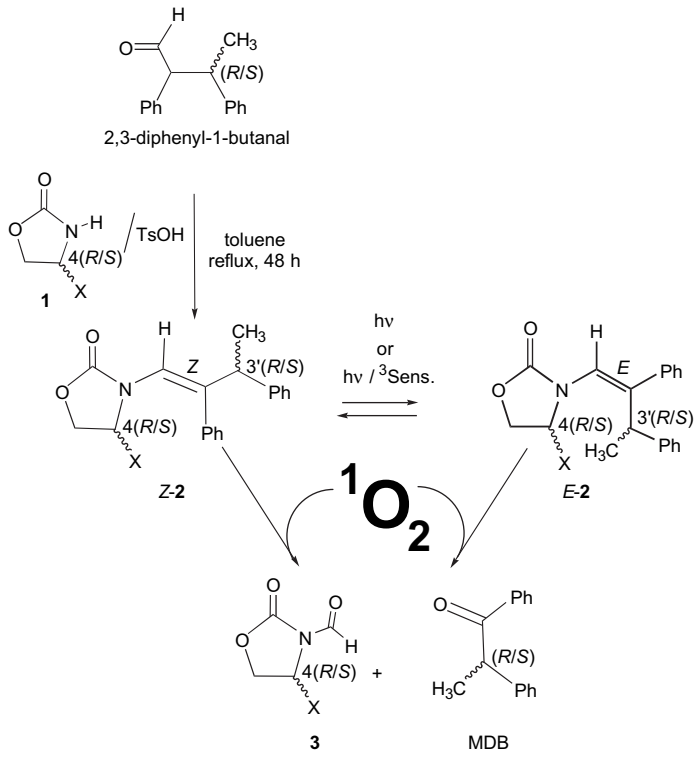

Scheme 2. Synthesis and photooxygenation of 4-oxazolidinone-functionalized *Z* and *E* enecarbamates.

to recover the starting material (*Z*-**2**). The slower running fraction was extracted with a 1:1 mixture of CH_2Cl_2 and EtOAc, to give 0.07 mmol of the corresponding *E*-**2**.

2.2.1.1. *E*(*R*)-2b. *E*(*R*)-**2b** was obtained in 95% yield according to the above general procedure. The two diastereomers 1′*E*,4*R*(Me),3′*R*-**2b** and 1′*E*,4*R*(Me),3′*S*-**2b** were separated on a preparative TLC plate by eluting with 2:1 hexane/methyl-*tert*-butyl ether mixture.

2.2.1.2. 1′*E*,4*R*(Me),3′*R*-2b. ^{1}H NMR (300 MHz, $CDCl_3$) δ^{ppm}=1.45 (d, *J*=6.10, 3H), 1.55 (d, *J*=7.14, 3H), 4.00 (m, 1H), 4.11 (m, 1H), 4.49 (m, 2H), 5.90 (s, 1H), 7.06 (m, 2H), 7.32 (m, 8H); ^{13}C NMR (75 MHz, $CDCl_3$) δ^{ppm}=16.9, 18.0, 39.4, 54.4, 120.7, 126.7, 127.4, 127.9, 128.3, 128.6, 129.4, 138.8, 143.6, 148.6, 157.1, 158.9; MS (FAB): M+H$^+$ Calcd 308.1572, Exptl 308.1644.

2.2.1.3. 1′*E*,4*R*(Me),3′*S*-2b. ^{1}H NMR (300 MHz, $CDCl_3$) δ^{ppm}=1.42 (d, *J*=5.93, 3H), 1.51 (d, *J*=7.23, 3H), 3.89 (m, 1H), 4.01 (m, 1H), 4.49 (m, 2H), 5.93 (s, 1H), 7.08 (m, 2H), 7.28 (m, 8H); ^{13}C NMR (75 MHz, $CDCl_3$) δ^{ppm}=17.4, 18.3, 54.6, 69.6, 121.2, 126.7, 127.5, 127.9, 128.2, 128.7, 129.5, 139.0, 143.6, 148.6, 159.0, 162.7; MS (FAB): M+H$^+$ Calcd 308.1572, Exptl 308.1656.

2.2.1.4. *E*(*R*)-2c. *E*(*R*)-**2c** was obtained in 95% yield according to the above general procedure. The two diastereomers 1′*E*,4*R*(^{i}Pr),3′*R*-**2c** and 1′*E*,4*R*(^{i}Pr),3′*S*-**2c** were separated on preparative TLC plate by eluting with 2:1 hexane/methyl-*tert*-butyl ether mixture.

2.2.1.5. 1′*E*,4*R*(^{i}Pr),3′*R*-2c. ^{1}H NMR (300 MHz, $CDCl_3$) δ^{ppm}=0.76 (d, *J*=7.03, 3H), 0.86 (d, *J*=6.85, 3H), 1.33 (d, *J*=7.20, 3H), 2.00–2.12 (m, 1H), 3.65 (ddd, *J*=8.10, 4.23, 3.66, 1H), 4.04 (dd, *J*=8.95, 4.33, 1H), 4.10 (t, *J*=8.68, 1H), 4.32 (q, *J*=7.20, 1H), 5.89 (s, 1H), 6.96–7.01 (m, 2H), 7.10–7.22 (m, 8H); ^{13}C NMR (75 MHz, $CDCl_3$) δ^{ppm}=14.6, 17.8, 18.4, 28.2, 39.2, 62.7, 63.1, 121.0, 126.3, 127.5, 127.6 (2C), 127.7 (2C), 128.2 (2C), 129.0 (2C), 138.9, 143.1, 146.1, 157.1; MS (FAB): M+H$^+$ Calcd 336.1958, Exptl 336.1972.

2.2.1.6. 1′*E*,4*R*(^{i}Pr),3′*S*-2c. ^{1}H NMR (300 MHz, $CDCl_3$) δ^{ppm}=0.87 (d, *J*=6.92, 6H), 1.39 (d, *J*=7.20, 3H), 2.01–2.15 (m, 1H), 3.75 (ddd, *J*=8.70, 4.78, 3.92, 1H), 4.08 (dd, *J*=8.95, 4.88, 1H), 4.19 (t, *J*=8.80, 1H), 4.28 (q, *J*=7.20, 1H), 5.88 (s, 1H), 6.84–6.87 (m, 2H), 7.07–7.27 (m, 8H); ^{13}C NMR (75 MHz, $CDCl_3$) δ^{ppm}=15.6, 17.3, 18.6, 29.5, 39.5, 63.2, 63.9, 121.9, 126.7, 127.9, 128.0 (4C), 128.7 (2C), 129.4 (2C), 138.4, 142.2, 144.9, 157.1; MS (FAB): M+H$^+$ Calcd 336.1958, Exptl 336.1961.

2.2.1.7. *E*(*S*)-2c. *E*(*S*)-**2c** was obtained in 95% yield according to the above general procedure. The two diastereomers 1′*E*,4*S*(^{i}Pr),3′*R*-**2c** and 1′*E*,4*S*(^{i}Pr),3′*S*-**2c** were on preparative TLC plate by eluting with 2:1 hexane/methyl-*tert*-butyl ether mixture.

2.2.1.8. 1′*E*,4*S*(^{i}Pr),3′*S*-2c. ^{1}H NMR (300 MHz, $CDCl_3$) δ^{ppm}=0.85 (d, 3H), 0.92 (d, 3H), 1.42 (d, 3H), 2.11–2.18 (m, 1H), 3.71–3.76 (ddd, 1H), 4.12 (dd, 1H), 4.19 (t, 1H), 4.41 (q, 1H), 5.97 (s, 1H), 7.06–7.11 (m, 2H), 7.20–7.34 (m, 8H); ^{13}C NMR (75 MHz, $CDCl_3$) δ^{ppm}=15.1, 18.5, 19.0, 28.2, 39.9, 62.9, 63.2, 121.4, 126.7, 127.9, 128.1 (4C), 128.7 (2C), 129.5 (2C), 138.9, 143.3, 146.6, 157.1; MS (FAB): M+H$^+$ Calcd 336.1958, Exptl 336.1952.

2.2.1.9. 1′*E*,4*S*(*i*Pr),3′*R*-2c. ^{1}H NMR (300 MHz, $CDCl_3$) δ^{ppm}=0.96 (d, 6H), 1.42 (d, 3H), 2.12–2.22 (m, 1H), 3.81–3.87 (ddd, 1H), 4.16 (dd, 1H), 4.28 (t, 1H), 4.37 (q, 1H), 5.96 (s, 1H), 6.93–6.97 (m, 2H), 7.16–7.35 (m, 8H); ^{13}C NMR (75 MHz, $CDCl_3$) δ^{ppm}=15.6, 17.3, 18.6, 29.5, 39.5, 63.2, 63.9, 121.9, 126.7, 127.9, 128.0 (4C), 128.7 (2C), 129.4 (2C), 138.4, 142.2, 144.9, 157.1; MS (FAB): M+H$^+$ Calcd 336.1958, Exptl 336.1950.

2.3. Instrumentation

GC analyses were carried out on a Varian 3900 gas chromatograph, equipped with an auto-sampler. A Varian Factor-4 VG-1ms column (l=25 m, id=0.25 mm, and df=0.25 μm) was employed for the separation on the achiral stationary phase, with a program of 50 °C for 4 min, raised to 225 °C at 10 °C min^{-1}, and kept at 225 °C for 10 min. A Varian CP-Chirasil-DEX CB column (l=25 m, id=0.25 mm, and df=0.25 μm) was used for the separation on the chiral stationary phase, with a program of 135 °C for 70 min, raised to 200 °C at 15 °C min^{-1}, and kept at 200 °C for 30 min. The ^{1}H NMR and ^{13}C NMR spectra were recorded on BRUKER spectrometers (Model DPX300 or DRX300).

2.3.1. Photooxygenation of *Z* and *E* enecarbamates (see Chart 1). The appropriate *Z* or *E* enecarbamate **2** (see Scheme 2) and methylene blue sensitizer in 0.7 mL of the desired deuterated solvent (the enecarbamate concentration was 3.0×10^{-3} M and that of methylene blue was 3.7×10^{-4} M) were placed into the NMR tube, sealed with a rubber septum, and fitted with a gas delivery needle and a vent needle. Dry O_2 gas was purged through the sample for 20 min, while irradiating with a 500-W halogen lamp, equipped with a cutoff filter (<500 nm). After irradiation, the samples were submitted to ^{1}H NMR spectroscopy to determine the conversion (kept below 50%). The mass balance (based on unreacted enecarbamate and formed MDB product) and the conversion (based on unreacted enecarbamate) were determined by GC analysis on an achiral stationary phase, with 4,4′-di-*tert*-butylbiphenyl as calibration standard. The enantioselectivity (% ee) of the MDB product was determined by GC analysis on a chiral stationary phase.

3. Results

To assess the diastereoselectivity in the oxidative cleavage of the chiral enecarbamate substrate *E*-**2** as a function of temperature and solvent, the photooxygenation under a variety of conditions was examined. Evans' chiral auxiliary[22,23] was chosen as the essential stereochemically directing entity and was introduced into the enecarbamate substrate *Z*-**2** by condensing the 4-alkyl-substituted oxazolidinones with the 2,3-diphenyl-1-butanal (see Scheme 2). The 1-phenylethyl substituent at the C-3′ position of the double bond was selected to minimize the *ene* reaction;[11,12,14–16] the required coplanar alignment of the only allylic hydrogen atom is encumbered. The *E*-**2** diastereomer was prepared by direct or sensitized photochemical isomerization of *Z*-**2**, followed by chromatographic separation (Scheme 2).[24] Analogous to the previously studied *Z* diastereomer,[13–15] the photooxygenation of the *E*-**2** enecarbamate gave the expected chiral methyldesoxybenzoin (MDB) and the oxazolidinone aldehyde **3** (see Scheme 2) quantitatively on complete conversion of the substrate. To recall, the thermally labile dioxetane intermediate was previously detected at −35 °C and was shown to decompose readily at room temperature (ca. 20 °C) into MDB and aldehyde **3**.[13–15]

To assess the diastereoselectivity in the oxidative cleavage of the chiral enecarbamate substrate *E*-**2** as a function of temperature and solvent, the photooxygenation under a variety of conditions was examined. The new results for the *E*-**2** diastereomers are collected in Table 1, together (for comparison purposes) with the relevant data of the already published *Z*-**2** diastereomers.[13–15] As for the previously studied *Z*-**2** diastereomers,[13–15] we employed a ca. 50:50 diastereomeric mixture of the *R* and *S* isomers at the C-3′ position also in the photooxygenations of the *E*-**2** enecarbamates. The conversion was kept below 50% to avoid overoxidation, which would therewith distort the ee values.

The negligible effect of the alkyl substituent at the oxazolidinone C-4 position in the photooxidative cleavage of the chiral enecarbamates **2** is exemplified for the *E* diastereomer with the methyl [*E*(*R*)-**2b**] and the isopropyl [*E*(*R*)-**2c**] groups (Table 1). In $CDCl_3$ at 18 °C the *E*(*R*)-**2b** (entry 2) gave the *R*-MDB enantiomer with an ee value of 67% at 19% conversion (s=5.9) and the *E*(*R*)-**2c** (entry 2) an ee value of 63% at 17% conversion (s=5.0). The respective s factors (see Eq. 1) convincingly express the relatively low response to the steric factors of the oxazolidinone chiral auxiliary. For this reason, hereafter we shall concentrate on the isopropyl derivative *E*-**2c**.

As already demonstrated previously for the *Z* series of diastereomers,[13–15] the sense of the enantioselectivity in the MDB product is opposite, while the extent of diastereomeric control in the photooxidative cleavage of the *E* enecarbamates is the same (within the experimental error) for the *R* and *S* antipodes at the C-4 position (Table 1). This is clearly evident in the % ee data for the *E*(*R*)-**2c** and *E*(*S*)-**2c** isomers, as exemplified by their photooxygenation in CD_2Cl_2 at 20 °C. As expected, the reversal in the enantioselectivity sense was also seen for *E*(*R*)-**2c** (entries 5–7) and affords the *S*-MDB (34% ee at 25% convn), whereas *E*(*S*)-**2c** (entries 17–19) leads to the *R*-MDB (28% ee at 29% convn) enantiomer as final oxidation products.

The effect of the solvent type and polarity was examined by comparing the polar aprotic solvent CD_3CN, the polar protic solvent CD_3OD, and the halogenated solvents CD_2Cl_2 and $CDCl_3$, which are of relatively low polarity. For the photooxidative cleavage of the *E*-**2c** substrate, the solvent dependence of the diastereoselectivity follows the order CD_3CN (30%)~CD_2Cl_2 (34%)<$CDCl_3$ (63%)<CD_3OD (85%) at the common temperature of about 18–20 °C (Table 1, entries 9, 5, 2 and 13, respectively); the ee values are given in parentheses. Evidently, the best diastereoselectivity is obtained for the hydrogen-bonding solvent methanol (entry 13), whereas the lowest control is displayed by the aprotic acetonitrile (entry 9) at the same temperature. The relatively high ee value in chloroform-*d* (entries 1–4) is quite striking. Mechanistically most revealing is the finding that the *R*-MDB enantiomer is the favored product in $CDCl_3$ and CD_3OD (entries 2 and 13, respectively), but the *S*-MDB isomer

Table 1. Determination of the stereoselectivity factor (*s*) for the formation of (*R*/*S*)-MDB product in the photooxygenation[a] of *E*(*R*)-**2b**, *E*(*R*)-**2c**, and *E*(*S*)-**2c** as a function of solvent and temperature

Entry	Temp (°C)	Solvent	MDB[b] (% ee)	Convn[c] (%)	*s*[d]	MDB[b] (% ee)	Convn[c] (%)	*s*[d]
			E(*R*)-**2b**			*E*(*R*)-**2c**		
1.	50	$CDCl_3$	—	—	—	8 (*S*)	5	1.2
2.	18		67 (*R*)	19	5.9	63 (*R*)	17	5.0
3.	−15		85 (*R*)	14	14.0	78 (*R*)	37	13.0
4.	−40		86 (*R*)	52	45.0	88 (*R*)	43	31.0
5.	20	CD_2Cl_2	7 (*S*)	10	0.9	34 (*S*)	25	2.3
6.	−20		62 (*R*)	23	5.1	27 (*R*)	65	2.7
7.	−60		95 (*R*)	31	59.0	82 (*R*)	54	40.0
8.	50	CD_3CN	—	—	—	64 (*S*)	23	5.5
9.	18		28 (*S*)	18	0.5	30 (*S*)	34	2.1
10.	−15		0	55	1.0	0	28	1.0
11.	−40		45 (*R*)	33	3.3	58 (*R*)	37	5.2
12.	50	CD_3OD	—	—	—	70 (*R*)	30	7.6
13.	18		75 (*R*)	17	8.1	85 (*R*)	34	19.0
14.	−15		80 (*R*)	13	10.0	90 (*R*)	17	23.0
15.	−40		86 (*R*)	13	15.0	94 (*R*)	12	37.0
16.	−70					97 (*R*)	8	72.0
						E(*S*)-**2c**		
17.	20	CD_2Cl_2				28 (*R*)	29	2.0
18.	−20					36 (*S*)	59	3.4
19.	−60					88 (*S*)	56	45.0

[a] The *E* enecarbamate concentration is 3.0×10^{-3} M and 3.7×10^{-4} M for the methylene blue sensitizer.
[b] The enantiomeric excess (% ee) of the MDB product, determined by GC analysis on a chiral stationary phase.
[c] Conversion (convn) of enecarbamates determined by GC analysis on an achiral stationary phase with 4,4′-di-*tert*-butylbiphenyl as calibration standard, and by ^{1}H NMR spectroscopy; averages of three runs, within 5% error of the stated values.
[d] Calculated from Eq. 1.

dominates in CD_2Cl_2 and CD_3CN (entries 5 and 9, respectively). Thus, the selectivity cannot be attributed to the solvent polarity alone in the photooxidative cleavage of the *E*-**2** enecarbamates.

Still more intriguing for mechanistic considerations is the temperature dependence of the ee values for the *E*-**2c** substrate (Table 1). Only in methanol the extent of the diastereoselectivity is relatively constant (note the high ee value of 97% at −70 °C, i.e., nearly perfect stereocontrol!) and the same enantiomer, namely *R*-MDB, is formed over the entire temperature range from −70 to +50 °C (entries 12–16). In the other solvents, depending on the temperature, a change in the sense from the usual *R*-MDB to the *S*-MDB isomer is observed. For example, very good stereocontrol (ee value of 88%) in favor of *R*-MDB is found in chloroform-*d* at −40 °C (entry 4), but the *S*-MDB isomer is preferred with very poor diastereoselectivity (ee value of only 8%) at +50 °C (entry 1). This inflection in the enantioselectivity sense (*R* to *S* isomer) occurs in $CDCl_3$ above +18 °C (entries

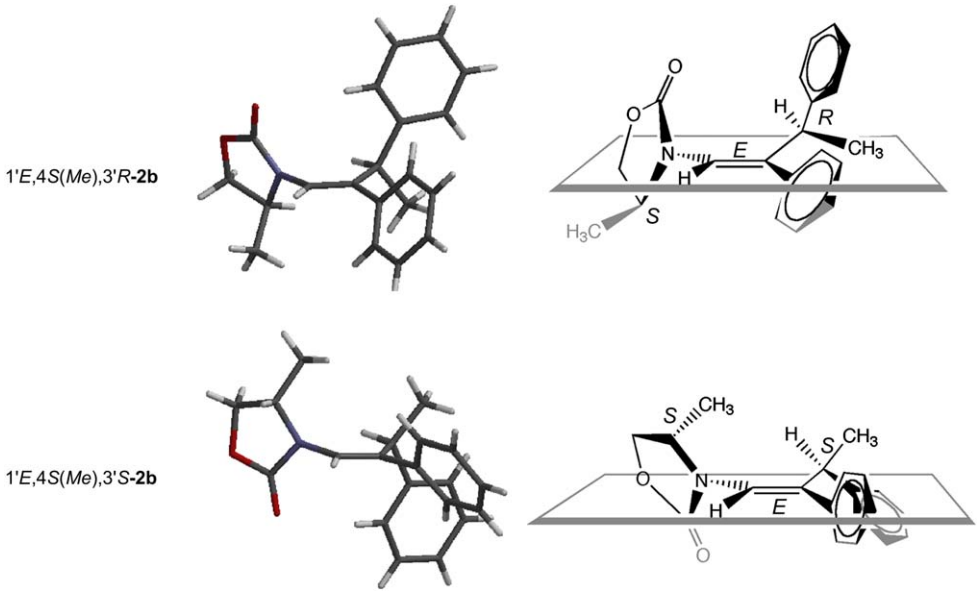

Figure 2. X-ray crystal structure (Ref. 25) of 1′*E*,4*S*(Me),3′*R*-**2b** and 1′*E*,4*S*(Me),3′*S*-**2b**.

1 and 2), while in CD_2Cl_2 it takes place between +20 °C and −20 °C (entries 5 and 6). In the case of CD_3CN, the temperature at which the change of sense takes place is −15 °C (entry 10), as indicated by the 0% ee value in the MDB product (see Table 1). These profound selectivity trends require careful mechanistic scrutiny, to understand the details of the photocleavage pathway.

To enable a detailed mechanistic rationalization of the favored attack by $^1O_2$ on the double bond of the enecarbamate, the structural details of the chiral enecarbamate must be known reliably. Fortunately, we succeeded in crystallizing the methyl derivative *E*(*S*)-**2b** from ether/hexane and obtained its solid-state structure by X-ray crystallography (Fig. 2).[25]

As displayed in Figure 2, both diastereomers 1′*E*,4*S*(Me),3′*R*-**2b** and 1′*E*,4*S*(Me),3′*S*-**2b** are contained in the same unit cell. Inspection of the crystal structure reveals that the oxazolidinone carbonyl is almost perpendicular to the plane of the double bond, such that the nitrogen lone pair is contained within that plane for conjugation with the carbonyl group. The phenyl substituent on the double bond is also twisted out of conjugation, to minimize the steric interactions with the phenethyl side chain. Presumably, polarity factors of the oxazolidinone functionality and steric interactions with the alkyl side chain are minimized in the observed conformation.

4. Discussion

The salient features of photooxygenation of the *E*-**2** and the *Z*-**2** diastereomers of the enecarbamates are three-fold:

(i) While the photooxidative cleavage of the *E*-**2** isomer affords the MDB product in high (up to 97%) enantioselectivity (Table 1), the ee value for the *Z*-**2** isomer is quite low (only 30% at best) under comparable reaction conditions;[11,12,14–16]

(ii) The enantiomeric excess in the MDB product depends substantially on the solvent and the temperature of the photooxygenation for the *E*-**2** isomer (Table 1), but that is not the case for the corresponding *Z*-**2** enecarbamate;[11,12,14–16]

(iii) Not only does the *extent* of stereoselection (% ee value) of the *E*-**2** diastereomer vary extensively as a function of solvent and temperature (Table 1), but also the favored configuration (*R* vs *S* enantiomers of MDB) changes, i.e., there is an inversion point in the *sense* of the stereoselectivity.

This divergent behavior in the stereocontrol displayed by the two geometrical isomers *E* and *Z* needs to be mechanistically rationalized in terms of the trajectory of the $^1O_2$ attack onto the double bond during the photooxidative cleavage of the enecarbamate substrate. Since we have employed for the photooxygenation a ca. 50:50 diastereomeric mixture of enecarbamates *E*-**2** (*R*/*S* epimers at the C-3′ stereogenic site of the alkyl side chain), the stereoselection in the present study entails a case of *kinetic resolution*. Thus, the enantiomeric excess in the MDB product, which is formed in the double-bond cleavage, reflects the differentiation in the reaction rates of the enecarbamate photooxidation. For such *kinetic resolution*, the so-called stereoselectivity factor (*s*) applies (Eq. 1),[26–29] which is a quantitative measure (corrected for the extent of conversion) of the relative reaction rates for the two stereoisomers in question. In the present photooxygenation of the enecarbamates **2**, the *s* factor for the two epimers from the substrate conversion and the MDB enantiomeric excess. A large value will translate into high enantiomeric excess in the MDB product even at 50% conversion (see Fig. 3). This is the case, for example, in the photooxidation of the *E*(*R*)-**2c** substrate in CD_3OD at −70 °C with the *s* factor of **72** (see Table 1, entry 16).

$$s = \frac{k_R}{k_S} = \frac{\ln[1 - C(1 + \mathrm{ee}_{\mathrm{MDB}})]}{\ln[1 - C(1 - \mathrm{ee}_{\mathrm{MDB}})]} \quad (1)$$

where *C* is the conversion and $\mathrm{ee}_{\mathrm{MDB}}$ is the ee value of the MDB product.

As a practical utilization of such a high *s* factor for the *kinetic resolution* with $^1O_2$, the photooxygenation of *E*(*R*)-**2c** was run in CD_3OD at −70 °C up to nearly 50% conversion. The *R*-MDB product was separated from the reaction mixture by chromatography and an ee value of 97% was obtained. The unreacted 1′*E*,4*R*(*i*Pr),3′*S*-**2c** enecarbamate was then quantitatively photooxidized at room temperature to afford the *S*-MDB product with an ee value of 97%. This remarkable case of $^1O_2$ stereoselection was previously coined as *photochemical Pasteur-type kinetic resolution*.[11,13,26–29]

To understand the temperature dependence of the enantiomeric excess in the MDB product for the photooxygenation of *E*(*R*)-**2c** in the various solvents, the differential activation parameters ($\Delta\Delta S^{\ddagger}$ and $\Delta\Delta H^{\ddagger}$) were computed with the help of Eyring relation (Eq. 2):[2,30,31]

$$\ln(k_R/k_S) = \Delta\Delta S^{\ddagger}_{R-S}/\mathrm{R} - \Delta\Delta H^{\ddagger}_{R-S}/\mathrm{R}T \quad (2)$$

The $\Delta\Delta S^{\ddagger}$ and $\Delta\Delta H^{\ddagger}$ data for the *E*(*R*)-**2b** and *E*(*R*)-**2c** diastereomers are collected in Table 2, together with the previously investigated *Z*(*R*)-**2c** in CD_2Cl_2 for comparison.[10]

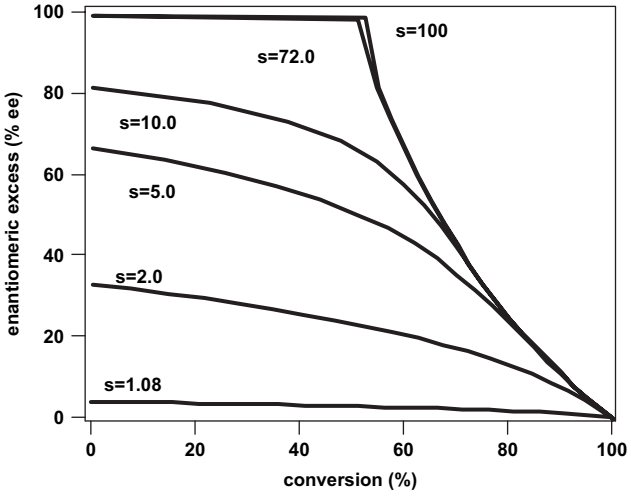

Figure 3. The dependence of the enantiomeric excess of the MDB product on the conversion of chiral oxazolidinone-functionalized enecarbamates as a function of the stereoselectivity factor (*s*).[26–29]

Table 2. Solvent dependence of the differential activation parameters[a] for the photooxygenation of *E*(*R*)-**2b**, *E*(*R*)-**2c**, *E*(*S*)-**2c**, and *Z*(*R*)-**2c** in different solvents

Entry	Solvent	$\Delta\Delta H^{\ddagger}$ (kcal mol^{-1})	$\Delta\Delta S^{\ddagger}$ (cal mol^{-1} K^{-1})	$\Delta\Delta H^{\ddagger}$ (kcal mol^{-1})	$\Delta\Delta S^{\ddagger}$ (cal mol^{-1} K^{-1})
		E(*R*)-**2b**		*E*(*R*)-**2c**	
1	$CDCl_3$	−4.9	−14	−4.5	−14
2	CD_2Cl_2	−6.6	−23	−4.0	−15
3	CD_3CN	−4.4	−17	−4.5	−17
4	CD_3OD	−1.5	−1.0	−2.5	−4.9
				E(*S*)-**2c**	
5	CD_2Cl_2			5.3	19.0
				Z(*R*)-**2c**	
6	CD_2Cl_2			−0.2	0.4

[a] $\Delta\Delta H^{\ddagger}$ and $\Delta\Delta S^{\ddagger}$ were computed from Eq. 2.

The data for the *E*-**2** isomer in the aprotic solvents $CDCl_3$, CD_2Cl_2, and CD_3CN display (Table 2, entries 1–3) a pronounced temperature dependence of the MDB enantiomeric excess, namely, a relatively high contribution by the differential activation entropy term ($|\Delta\Delta S^{\ddagger}| \geq 14$ cal mol^{-1} mol^{-1}), as well as an appreciable contribution by the differential activation enthalpy term ($|\Delta\Delta H^{\ddagger}| \sim 4$ kcal mol^{-1}). As may be seen from the differential Eyring relation (Eq. 2), the change in the % ee values (or $\Delta\Delta G^{\ddagger}$) depends both on the entropic and enthalpic terms. Since the $\Delta\Delta H^{\ddagger}_{R-S}/RT$ term is proportional to the reciprocal temperature (Eq. 2), the $\ln(k_R/k_S)$ value is determined mostly by the enthalpic contribution at low temperatures; however, as the temperature increases, the relative contribution from the $\Delta\Delta S^{\ddagger}_{R-S}/R$ term increases and begins to override the $\Delta\Delta H^{\ddagger}_{R-S}/RT$ term at some temperature. Eventually, the sign of the $\ln(k_R/k_S)$ value inverts and the enantioselectivity sense switches, provided that the $\Delta\Delta H^{\ddagger}_{R-S}$ and $\Delta\Delta S^{\ddagger}_{R-S}$ terms possess the same sign, as is the case here for the photooxygenation of the *E*-**2** isomer (Table 2, entries 1–3). Such entropy effects are indicative of conformational factors,[2,30,31] which in the present case are dictated, presumably, by the stereogenic center at the C-3′ position of the phenethyl side chain.

In contrast, the corresponding *Z*-**2c** isomer is insensitive to temperature, as convincingly exposed by the near-zero $\Delta\Delta S^{\ddagger}$ and $\Delta\Delta H^{\ddagger}$ terms in CD_2Cl_2 with opposite sign (Table 2, entry 6);[2,30,31] consequently, irrespective of what temperature is chosen, the *R*-enantiomeric MDB product is enhanced (as $\Delta\Delta S^{\ddagger}$ and $\Delta\Delta H^{\ddagger}$ compensate each other upon temperature variations due to the opposite sign), but in modest preference. Similarly, in the protic CD_3OD solvent, also for the *E*-**2** isomer a small temperature dependence is observed (Table 1, entries 12–16), again corroborated by the small $\Delta\Delta S^{\ddagger}$ and $\Delta\Delta H^{\ddagger}$ values (Table 2, entry 4). As a consequence of the low entropy and enthalpy contributions, in the protic methanol (notice the same sign for $\Delta\Delta S^{\ddagger}$ and $\Delta\Delta H^{\ddagger}$; upon decreasing the temperature the contribution from $\Delta\Delta H^{\ddagger}$ will increase slightly), the response of the *E*-**2** isomer to temperature is nominal; certainly the sense of the enantioselectivity is not changed.

An effective visual display of these experimental trends in the temperature dependence of k_R/k_S as a function of the solvent nature is given in Eyring plots for *E*-**2c** (Fig. 4). The

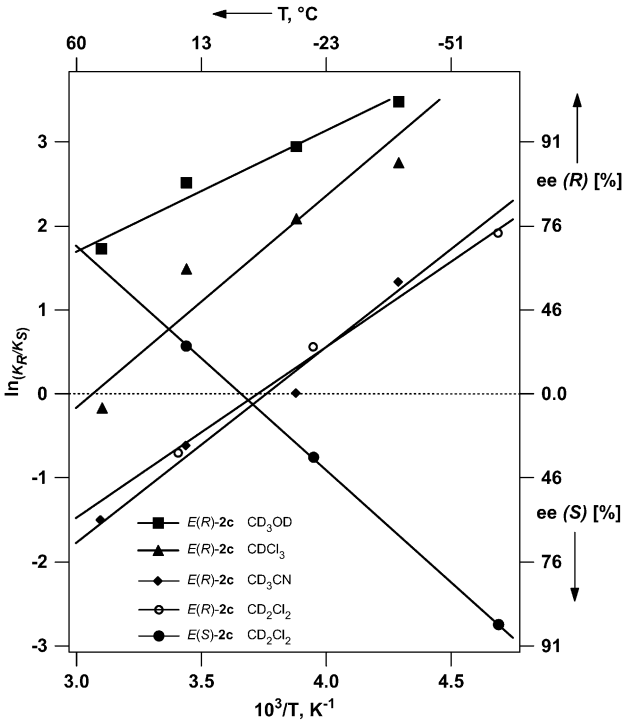

Figure 4. Eyring plots for the stereoselective photooxygenation of *E*(*R*)-**2c** and *E*(*S*)-**2c** enecarbamates in various solvents.

nearly parallel lines (similar slopes) bring out the fact that the extent of enthalpic contribution ($\Delta\Delta H^{\ddagger}$) is about the same as that in the diverse solvents, but the crossing of the 0% ee line reflects the change in the sense of specification of the favored configuration for the MDB enantiomer. Another point that is focused well in Figure 4, is the mirror imaging of the two lines for the *E*(*R*)-**2c** [–○–] and *E*(*S*)-**2c** [–●–] diastereomers upon photooxygenation in CD_2Cl_2, which conveys the stereocontrol by the stereogenic center at the C-4 position of the oxazolidinone chiral auxiliary. The similar magnitudes but opposite signs of the $\Delta\Delta S^{\ddagger}$ and $\Delta\Delta H^{\ddagger}$ terms for the oppositely configured *E*(*R*)-**2c** and *E*(*S*)-**2c** diastereomers in CH_2Cl_2 (Table 2; entries 2 and 5, respectively) are dictated by mirroring of the two lines in Figure 4. The intersection of the two lines signifies the temperature (*inversion* temperature, −3 °C for CD_2Cl_2) at which the entropic contribution equals the enthalpic contribution, which will be reflected in the 0% ee value in the MDB product.

These conspicuously complex temperature and solvent effects on the stereoselectivity of the *E* and *Z* enecarbamate photooxygenation shall now be mechanistically scrutinized. As already anticipated, conformational factors may be responsible for the difference in the sensitivity response between the *E* and *Z* oxazolidinone-functionalized enecarbamates toward solvent and temperature variations. To assess such conformational factors, detailed X-ray crystal structures of the *E* and *Z* diastereomers should be helpful; however, such structures are not necessarily definitive, since our photooxygenations are conducted in the solution phase and not in the solid state, for which the actual conformations may differ appreciably. The pertinent crystal structures are given in Figure 5, which disclose some significant conformational differences.

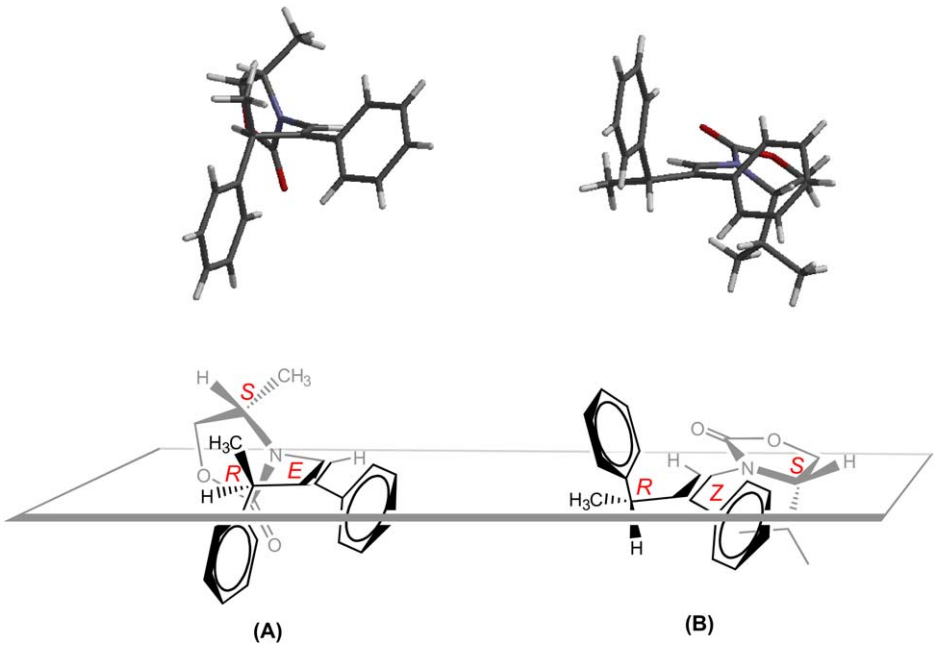

Figure 5. Comparison of the favored conformers for the *E*-4*S*(Me),3′*S*-**2b** (**A**) and *Z*-4*S*(ⁱPr),3′*S*-**2c** (**B**) enecarbamates, as revealed by the corresponding solid-state structures, of the *E*-4*S*(Me),3′*S*-**2b** (A) and *Z*-4*S*(ⁱPr),3′*S*-**2c** (B) enecarbamates (for clarity, only the 4*R*,3′*S* epimers are shown), which disclose some pertinent conformational differences. It should, however, be emphasized that in (A) we are using the *methyl* derivative, whereas in (B) the *isopropyl* one; unfortunately, the crystal structures are not available for the same alkyl group at the C-4 position of the oxazolidinone chiral auxiliary; nevertheless, for the present discussion it is not the substituent in the oxazolidinone chiral auxiliary that counts, but the *E* and *Z* geometries of the double bond.

As illustrated in Figure 5, the oxazolidinone carbonyl of the *E* isomer (C-3′*S* epimer) is oriented above the plane of the double bond (for the other C-3′*R* epimer, the oxazolidinone carbonyl is oriented below),[25] compared to the coplanar alignment of the *Z* isomer (see Fig. 5).[13–15] Moreover, molecular models and quantum-chemical computations suggest that the *Z* diastereomer[13–15] is conformationally more rigid than the *E* one. The greater flexibility of the *E* conformer appears to be due to less steric encumbrance between the imposing phenyl and oxazolidinone groups. Therefore, we speculate that the more mobile *E* conformer is more susceptible to solvent and temperature variations, as confirmed by the larger $\Delta\Delta S^{\ddagger}$ contribution (Table 2). Correspondingly, the greater rigidity of the *Z* conformer makes it less sensitive to solvent and temperature variations, as reflected by the lower $\Delta\Delta S^{\ddagger}$ values (Table 2). Further work would be required, to confirm the higher flexibility of the *E* conformer, e.g., NOESY and NOE NMR spectroscopy as well as theoretical studies would be helpful.

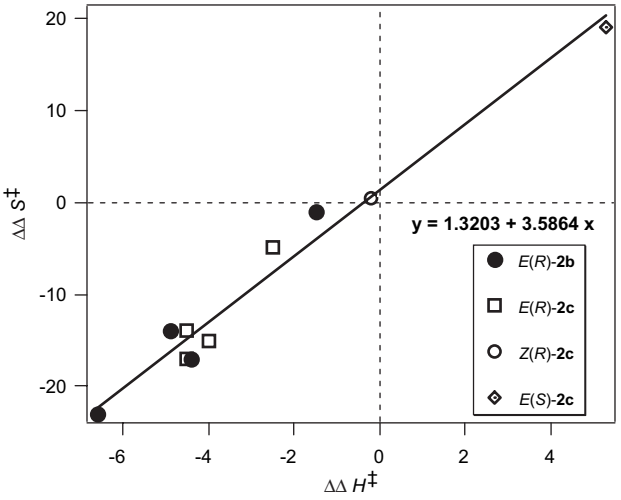

Figure 6. Plot of $\Delta\Delta S^{\ddagger}$ versus $\Delta\Delta H^{\ddagger}$ for the photooxygenation of *E*(*R*)-**2b**, *E*(*R*)-**2c**, *E*(*S*)-**2c**, and *Z*(*R*)-**2b**.

The enthalpy–entropy plot for both the *E* and *Z* enecarbamates is shown in Figure 6. The differential activation parameters fall on a single straight line passing through the origin, which indicates that the same diastereo-differentiating mechanism operates, irrespective of (a) the configuration of the double bond [*E* or *Z*], (b) the alkyl substituent at the C-4 position [Me or ⁱPr], (c) the configuration of the C-4 substituent [*R* or *S* isomer], and (d) the solvent that is employed.

A pertinent aspect to be rationalized is the higher stereoselectivity of the *E* compared to the *Z* enecarbamate. It is truly remarkable that the smallest possible oxidant, namely *singlet oxygen*, is subject to such high stereocontrol. To understand the higher stereocontrol for the *E* isomer, we shall explore now the details of the trajectory for the incoming $^1O_2$ onto the double bond of the chiral enecarbamate, to reveal the critical oxidant/substrate interactions in the attack. As exemplified in Figure 2, the configuration at the C-3′ position, i.e., 3′*R* versus 3′*S*, plays an important role in aligning the oxazolidinone carbonyl with respect to the face of the double bond. In 1′*E*,4*S*(Me),3′*R*-**2b**, the oxazolidinone carbonyl is oriented toward the top face of the double bond, whereas in the 1′*E*,4*S*(Me),3′*S*-**2b** epimer it is steered toward the bottom face. Although it is well known that polar groups may facilitate the facial selectivity of singlet oxygen,[32] in the present case, this alone does not explain the high selectivity for the *E* isomer. The reason is that the relative spatial arrangement of the carbonyl and the phenethyl groups is the same in both the structures and, thus, equal

amounts of the *R*- and *S*-MDB enantiomers would be expected. Evidently, besides conformational and steric factors, additional interactions must be involved.

We propose that the high stereocontrol in the *R*-MDB versus *S*-MDB formation for the photooxidative cleavage of the *E* isomer is the consequence of selective π-facial quenching of the electronically excited singlet oxygen by the enecarbamate substrate. In this context, it is well known that the lifetime of singlet oxygen in deuterated solvents is much higher than non-deuterated ones,[17–20] since C–H bond vibrations deactivate $^1O_2$ to its triplet ground state.[33] In view of the higher flexibility of *E* enecarbamates, conformations may be populated, in which one π face of the double bond exposes a larger number of C–H bonds for selective quenching[33] of the incoming excited $^1O_2$. In the present case of *kinetic resolution*, to generate selectively the *R*-MDB enantiomer in excess from the 3′*R*/3′*S* diastereomeric pair, the 3′*S* epimer must be preferentially quenched and thereby accumulates. We have previously shown low selectivity in the MDB product for photooxidation of both *E* and Z enecarbamates with ozone—a reactive ground state species.[34] A more careful inspection of the solid-state structures for the 3′*R*/3′*S* diastereomeric pair in Figure 2 reveals that in the 3′*R* epimer, the methyl groups of the oxazolidinone ring and the phenethyl side chain are located on opposite π faces of the double bond, whereas in the 3′*S* epimer these methyl groups are on the same side (in the shown structure, above the plane of the double bond). If such conformationally imposed structural differences apply also in the solution phase, the attacking $^1O_2$ is more efficiently deactivated by the 3′*S* epimer and the *R*-MDB enantiomer is favored, as observed in aprotic solvents at subambient temperature (Table 1). The more efficient stereocontrol (higher % ee values in favor of the *R*-MDB enantiomer) as the temperature is decreased (Table 1), may arise from populating in solution, the favored conformations of the 3′*R*/3′*S* diastereomeric pair. Consequently, at the lower temperature limit, the *R*-MDB enantiomer is favored due to more effective $^1O_2$ quenching, whereas at the higher temperature limit the proportion of *S*-MDB product increases because the mechanism of selective π-facial quenching is depreciated as a result of efficient conformational equilibration. In the latter situation, presumably steric effects override physical deactivation of the electronically excited $^1O_2$. Evidently, the complex stereoselectivity behavior presently observed in the photooxidative cleavage of the chiral enecarbamates **2** (Table 1, Fig. 4) is a delicate balance between the steric interactions and quenching in the $^1O_2$/substrate encounter, imposed by temperature-dependent and solvent-dependent conformational preferences.

5. Conclusion

It should be evident that the extensive stereochemical properties embodied in the chiral oxazolidinone-substituted enecarbamates (i.e., the chirality center at the C-4 position of the oxazolidinone ring, the chirality center at the C-3′ position of the phenethyl side chain, and the *E*/*Z* configurations of the alkene functionality) make these substrates informative molecular probes to explore the mechanistic intricacies of kinetic resolution in the photooxidative cleavage of the alkenyl double bond to the enantiomerically enriched MDB. The stereoselection of the kinetically preferred MDB enantiomer depends not only on the alkene geometry (*Z*/*E*), the size of the C-4 alkyl substituent (H, Me, ^{i}Pr) in the oxazolidinone ring, and the configuration (*R*/*S*) at the C-3′ stereogenic center of the phenethyl side chain, but also on the nature of the solvent and the reaction temperature. The conformationally more flexible *E* diastereomer responds sensitively to such reaction conditions (ee values of up to 97%), whereas the conformationally more rigid *Z* diastereomer behaves impervious to such manipulation (ee values of up to 30%). We argue that the stereochemical consequences of such conformational effects (entropy control) are stereoselective quenching of $^1O_2$ by vibrational deactivation (a novel concept), in competition with stereoselective oxidative double-bond cleavage subject to steric interactions on the attacking $^1O_2$.

Acknowledgements

The authors at Columbia thank the NSF (CHE 01-10655 and CHE-04-15516) for generous support of this research. W.A. is grateful for the financial support from the Deutsche Forschungsgemeinschaft, Alexander-von-Humboldt Stiftung, and the Fonds der Chemischen Industrie. T.P. acknowledges the support of the W.M. Keck Foundation. H.S. and Y.I. gratefully acknowledge a JSPS research for fellowship for young scientists (08384) for young scientists to H.S. The authors thank Dr. Sara G. Bosio for initiating the work on the photooxygenation of *Z* enecarbamates.

References and notes

1. Inoue, Y.; Ramamurthy, V. *Chiral Photochemistry*; Marcel Decker: New York, NY, 2004; pp 685.
2. Inoue, Y. *Chem. Rev.* **1992**, *92*, 741–770.
3. Rau, H. *Chem. Rev.* **1983**, *83*, 535–547.
4. Turro, N. J. *Proc. Natl. Acad. Sci. U.S.A.* **2002**, *99*, 4805–4809.
5. Turro, N. J.; Cheng, C. C.; Abrams, L.; Corbin, D. R. *J. Am. Chem. Soc.* **1987**, *109*, 2449–2456.
6. Ramamurthy, V. *Photochemistry in Organized and Confined Media*; Wiley-VCH: New York, NY, 1991.
7. Garcia-Garibay, M. A. *Acc. Chem. Res.* **2003**, *36*, 491–498.
8. Sivaguru, J.; Natarajan, A.; Kaanumalle, L. S.; Shailaja, J.; Uppili, S.; Joy, A.; Ramamurthy, V. *Acc. Chem. Res.* **2003**, *36*, 509–521.
9. Sivaguru, J.; Shailaja, J.; Uppili, S.; Ponchot, K.; Joy, A.; Arunkumar, N.; Ramamurthy, V. Achieving Enantio and Diastereoselectivities in Photoreactions Through the Use of a Confined Space. In *Organic Solid-State Reactions*; Toda, F., Ed.; Kluwer Academic: Dordrecht, The Netherlands, 2002; pp 159–188.
10. Poon, T.; Turro Nicholas, J.; Chapman, J.; Lakshminarasimhan, P.; Lei, X.; Adam, W.; Bosio Sara, G. *Org. Lett.* **2003**, *5*, 2025–2028.
11. Poon, T.; Sivaguru, J.; Franz, R.; Jockusch, S.; Martinez, C.; Washington, I.; Adam, W.; Inoue, Y.; Turro, N. J. *J. Am. Chem. Soc.* **2004**, *126*, 10498–10499.
12. Sivaguru, J.; Poon, T.; Franz, R.; Jockusch, S.; Adam, W.; Turro, N. J. *J. Am. Chem. Soc.* **2004**, *126*, 10816–10817.
13. *Chem. Eng. News* **2004**, *82*, 7.
14. Adam, W.; Bosio, S. G.; Turro, N. J. *J. Am. Chem. Soc.* **2002**, *124*, 14004–14005.

15. Adam, W.; Bosio, S. G.; Turro, N. J. *J. Am. Chem. Soc.* **2002**, *124*, 8814–8815.
16. Adam, W.; Bosio, S. G.; Turro, N. J.; Wolff, B. T. *J. Org. Chem.* **2004**, *69*, 1704–1715.
17. Wasserman, H. H.; Murray, R. W. *Singlet Oxygen*; Academic: New York, NY, 1979.
18. Gollnick, K.; Kuhn, H. J. *Singlet Oxygen*; Wasserman, H. H., Murray, R. W., Eds.; Academic: New York, NY, 1979.
19. Foote, C. S. *Acc. Chem. Res.* **1968**, *1*, 104–110.
20. Frimer, A. A. *Singlet Oxygen*; CRC: Boca Raton, 1985; Vol. 1–4.
21. Poon, T.; Turro, N. J.; Chapman, J.; Lakshminarasimhan, P.; Lei, X.; Jockusch, S.; Franz, R.; Washington, I.; Adam, W.; Bosio, S. G. *Org. Lett.* **2003**, *5*, 4951–4953.
22. Evans, D. A.; Bartroli, J.; Shih, T. L. *J. Am. Chem. Soc.* **1981**, *103*, 2127–2129.
23. Ager, D. J.; Prakash, I.; Schaad, D. R. *Chem. Rev.* **1996**, *96*, 835–876.
24. Saito, H.; Sivaguru, J.; Jockusch, S.; Inoue, Y.; Adam, W.; Turro, N. J. *Chem. Commun.* **2005**, 3424–3426.
25. Detailed X-ray structure analysis of the *E* enecarbamates will be published elsewhere.
26. Kagan, H. B.; Fiaud, J. C. *Top. Stereochem.* **1988**, *18*, 249–330.
27. Keith, J. M.; Larrow, J. F.; Jacobsen, E. N. *Adv. Synth. Catal.* **2001**, *343*, 5–26.
28. Martin, V. S.; Woodward, S. S.; Katsuki, T.; Yamada, Y.; Ikeda, M.; Sharpless, K. B. *J. Am. Chem. Soc.* **1981**, *103*, 6237–6240.
29. Chen, C. S.; Fujimoto, Y.; Girdaukas, G.; Sih, C. J. *J. Am. Chem. Soc.* **1982**, *104*, 7294–7299.
30. Buschmann, H.; Scharf, H.-D.; Hoffmann, N.; Esser, P. *Angew. Chem., Int. Ed. Engl.* **1991**, *30*, 477–515.
31. Otera, J.; Sakamoto, K.; Tsukamoto, T.; Orita, A. *Tetrahedron Lett.* **1998**, *39*, 3201–3204.
32. Prein, M.; Adam, W. *Angew. Chem., Int. Ed. Engl.* **1996**, *35*, 471–494.
33. Turro, N. J. *Tetrahedron* **1985**, *41*, 2089–2098.
34. Sivaguru, J.; Saito, H.; Poon, T.; Omonuwa, T.; Franz, R.; Jockusch, S.; Hooper, C.; Inoue, Y.; Adam, W.; Turro, N. J. *Org. Lett.* **2005**, *7*, 2089–2092.